ACS APPLIED MATERIALS & INTERFACES

RESEARCH ARTICLE

www.acsami.org

Fabrication of Graphene Thin Films Based on Layer-by-Layer Self-Assembly of Functionalized Graphene Nanosheets

Je Seob Park,[†] Sung Min Cho,[‡] Woo-Jae Kim,[∥] Juhyun Park,[§] and Pil J. Yoo*[,†,‡]

[†]SKKU Advanced Institute of Nanotechnology (SAINT) and [‡]School of Chemical Engineering, Sungkyunkwan University, Suwon 440-746, Republic of Korea

[∥]Division of Energy and Biological Engineering, Kyungwon University, Sungnam 461-701, Republic of Korea

[§]School of Chemical Engineering and Materials Science, Chung-Ang University, Seoul 151-756, Republic of Korea

ABSTRACT: In this study, we present a facile means of fabricating graphene thin films via layer-by-layer (LbL) assembly of charged graphene nanosheets (GS) based on electrostatic interactions. To this end, graphite oxide (GO) obtained from graphite powder using Hummers method is chemically reduced to carboxylic acid-functionalized GS and amine-functionalized GS to perform an alternate LbL deposition between oppositely charged GSs. Specifically, for successful preparation of positively charged GS, GOs are treated with an intermediate acyl-chlorination reaction by thionyl chloride and a subsequent amidation reaction in pyridine, whereby a stable GO dispersibility can be maintained within the polar reaction solvent. As a result, without the aid of additional hybridization with charged nanomaterials or polyelectrolytes, the oppositely charged graphene nanosheets can be electrostatically assembled to form graphene thin films in an aqueous environment, while obtaining controllability over film thickness and transparency. Finally, the electrical property of the assembled graphene thin films can be enhanced through a thermal treatment process. Notably, the introduction of chloride functions during the acyl-chlorination reaction provides the p-doping effect for the assembled graphene thin films, yielding a sheet resistance of 1.4 kΩ/sq with a light transmittance of 80% after thermal treatment. Since the proposed method allows for large-scale production as well as elaborate manipulation of the physical properties of the graphene thin films, it can be potentially utilized in various applications, such as transparent electrodes, flexible displays and highly sensitive biosensors.

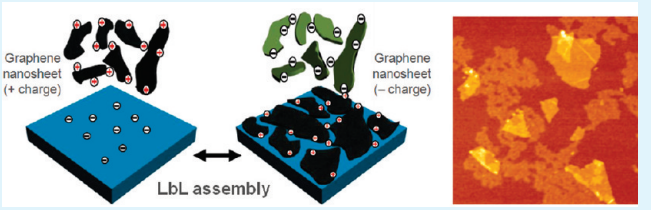

KEYWORDS: graphene, graphite oxide, nanosheets, layer-by-layer assembly, thionyl chloride, doping, transparent electrodes

INTRODUCTION

Although less than a decade has passed since graphene was first introduced, it has received much attention in numerous areas ranging from academic research to practical device application. Because of its structural homogeneity and physical stability, graphene has outstanding electrical properties and has been used in several demonstrations of next-generation electronic devices.[1−3] To produce graphene, various approaches have been used including chemical vapor deposition (CVD) of methane gas,[4−6] graphite oxide reduction,[7,8] one-step graphite exfoliation,[9] graphite stamping,[10] and carbon nanotube unzipping.[11,12] Among these, a means of obtaining graphite oxide (GO) from graphite powder and its further reduction to graphene has been extensively studied due to its ease of fabrication and economic feasibility. Several approaches have been suggested for the reduction of GO, such as chemical,[7,8,13−15] thermal,[16,17] and ultraviolet-assisted reduction methods.[18] The chemical reduction method is advantageous in that a large amount of GO in the solution phase can be readily converted to graphene nanosheets (GS) through the removal of epoxide groups present on the basal plane of GO via a hydrazine reduction.[19]

Similar to the successful demonstration of large-scale epitaxial preparation of graphene thin films using a CVD method based on direct carbon deposition onto the substrate, the graphene nanosheets chemically prepared from GO can be assembled and integrated into a thin film for various applications. With this goal in mind, recent studies have focused on expanding the chemical functionalities of graphene by enhancing its solvent solubility or by attaching multiple functional groups onto the GSs.[20−22] Various methods have been proposed for the construction of a large-scale assembled graphene film, utilizing a strategy of bottom-up based self-assembly of functionalized GSs, such as Langmuir−Blodgett (LB) film assembly,[23,24] vacuum filtration (graphene paper),[25−27] or an air−water interface collection method.[28] However, the assembled graphene film prepared through LB assembly lacks film uniformity because of the incompletely interconnected networks between monolayer assembled GSs. Other methods are also limited by their lack of precise control of film thickness.

Received: October 10, 2010
Accepted: December 15, 2010
Published: January 5, 2011

As an efficient route for generating large-scale structured functional films in an aqueous environment, the layer-by-layer (LbL) assembly of charged nanomaterials can be considered as a promising candidate, in which the electrostatic attractive interactions between oppositely charged polyelectrolytes are employed to create function-embedded polymeric thin films.[29,30] In recent studies, various other types of charged materials, such as inorganic nanoparticles,[31,32] biomolecules,[33,34] or carbon nanotubes (CNT)[35] have been used in the fabrication of hybridized functional thin films using LbL assembly. In particular, for LbL self-assembly of CNTs, functionalized CNTs whose surfaces were modified with either carboxylic acid or amine groups were alternately applied for construction of all-CNT assembled films.[36] Therefore, this successful demonstration of LbL assembly of one-dimensional CNTs provided a motivation for an extended application to two-dimensional graphene materials.

It has been reported that carboxylic acid-functionalized GS could be complexed with positively charged polyelectrolytes or nanoparticles.[37−40] Indeed, an ordered nanostructure formed through the hybridization between negatively charged GSs and positively charged CNTs has been suggested.[41] However, because the assembly process has mostly relied on a heterogeneous electrostatic complexation between negatively charged GS and other positively charged auxiliary species, strategic extension to a broad range of materials was severely restricted. Therefore, to provide a positively charged characteristic for GS, attempts have been made to mix a positively charged dispersing agent with GS, followed by an LbL assembly process with negatively charged polyelectrolytes for construction of an ionically complexed thin film.[42,43] In addition to this indirect approach, a noteworthy direct method of attaching the positively charged amine functionality onto the GO surface has been suggested. However, most of the positively charged graphenes were dispersed in organic solvents and only a few studies were reported for the dispersibility in aqueous condition.[44−46] The greatest challenge in the fabrication of water dispersible and positively charged GS can be attributed to the repeated sample drying steps in the course of synthesis, which leads to the permanent aggregation of GSs.

On the basis of our understanding of these technical needs, we present the synthesis of water-dispersible, positively charged GS via sequential functionalization processes of acyl-chlorination by thionyl chloride and amidation by ethylenediamine. Because thionyl chloride has a very strong reactivity with oxygen, the epoxide groups on the basal plane of GS are prone to dissociation by thionyl chloride in the course of the acyl-chlorination, likely causing surface defects and deformations in the GS. However, this structural deficiency could advantageously mitigate the concern of GS aggregation during the midprocess of sample drying, because the drying-induced molecular interactions in the proximity may be negated. Furthermore, when considering the high polarity of the acyl chlorinated GS of the reaction intermediate, a subsequent amidation process is performed in pyridine, which is an environment of polar organic solvent; this results in successful synthesis of the amine-functionalized and positively charged GS, while allowing for stable dispersibility in the aqueous environment.

As a result, to create the chemically self-assembled graphene thin films, the positively charged GS are alternately complexed with the negatively charged GS through an electrostatic LbL process. Simply by varying the number of LbL depositions, the physical properties of the constructed thin films, such as film thickness or optical transparency, can be readily manipulated. Finally, a further thermal annealing process can convert the LbL-assembled GS film to the graphene film of the purified condition, yielding a low sheet resistance with a kilo-ohm/sq. Although a slight structural deficiency is inherent to the positively charged GS, this can be compensated for through the structural intactness of the negatively charged GS during the complexation process of the LbL assembly, in such a way that the loss in electrical conductivity of the assembled graphene films can be effectively minimized. In addition, the acyl-chlorination reaction by thionyl chloride adopted in the midstep of the amine functionalization process of GS can provide a p-doping effect to the assembled graphene films, promoting the electrical conductivities of the reduced graphene thin films.

EXPERIMENTAL SECTION

Preparation of Negatively and Positively Charged Graphene Nanosheets (GSs). First, graphene oxide (GO) was prepared from graphite powder (<20 μm, synthetic, Aldrich) using a modified Hummers method.[47] To synthesize the carboxylic acid-functionalized graphene nanosheet (GS) dispersion (approximately 0.05 wt %), GOs were mixed with hydrazine (35 wt %, Aldrich) at a ratio of 7:10, and the chemical reduction reaction proceeded at 80 °C for 1 h. In parallel, to synthesize the amine-functionalized GS dispersion, GOs prepared via Hummers method were not exfoliated by sonication but were instead left to dry completely at 50 °C in a vacuum and collected as a powder phase. To promote the acyl-chlorination reaction of dried GOs, an intermediate process for the final amidation reaction, we added an excess amount of thionyl chloride ($SOCl_2$, Samchun Pure Chemical Co., Korea) to GOs and reacted it with refluxing at 70 °C for 12 h, after which the remaining thionyl chloride was removed by drying. For amidation, ethylenediamine (>99%, Sigma-Aldrich) was added to acyl chlorinated GSs and reacted in pyridine (anhydrous, >99.8%, Sigma-Aldrich) solution at 80 °C for 1 day. After the reaction was completed, the reaction products were repeatedly rinsed with methanol and deionized (DI) water and finally exfoliated using sonication (ULH700S, Ulsso Hitech Co., Korea) for 30 min. Nonexfoliated amine-functionalized GSs were removed via centrifugation (5804R, Eppendorf, Germany), and amine-functionalized GSs were redispersed in DI water at a targeted concentration (0.05 wt %).

Layer-by-Layer Assembly of Charged Graphene Nanosheets. Quartz substrates were first cleaned with sonication in DI water and ethanol, then the substrates were plasma-treated (<30 W, 0.1−0.5 Torr, PDC-001, Harrick Scientific Corp., NY) for one minute to produce a negatively charged surface. The layer-by-layer assembly of charged GSs was performed using a programmable slide stainer (HMS70, Microm, Germany) with a deposition condition of eight minutes adsorption of charged GSs, followed by three sequential washing steps in a DI water bath. To compensate for the negative charge of the substrate, positively charged GS was initially adsorbed, and then negatively charged GS was alternately applied to produce an electrostatic bond (see Figure 1). The notation of GS_X will be used to denote a multilayer film of X layered pairs of GSs. When X includes 0.5, positively charged GS is the final adsorbed outermost layer. The alternate depositions of GS were repeated until the targeted thickness of the assembled films was attained. Finally, the assembled graphene film was thermally reduced in a furnace in an inert environment with argon purging. The annealing temperature was varied between 300 and 900 °C.

Characterization of LbL-Assembled Graphene Thin Films. The surface charge density of the synthesized GS was characterized according to a zeta potential measurement (ELS-Z, Otsuka Electronics Co., Japan). The atomic composition and chemical structures of synthesized GSs were characterized with an energy dispersive spectrometer

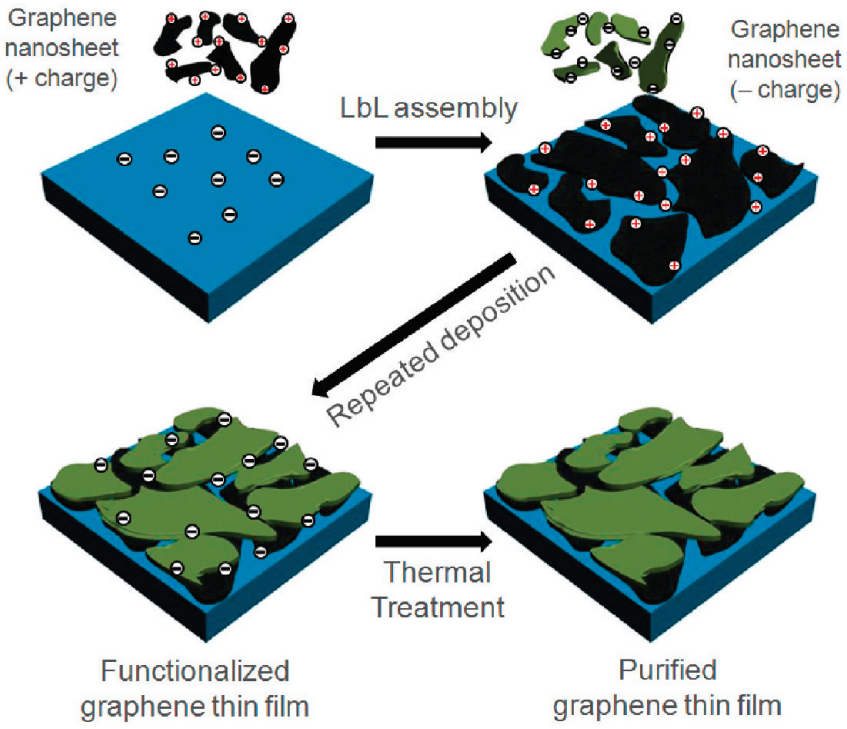

Figure 1. Schematic illustration of the generation of graphene thin films using an electrostatic layer-by-layer (LbL) assembly between oppositely charged graphene nanosheets and subsequent thermal treatment.

(EDS, INCAPentaFET-X3, Oxford, U.K.) and Fourier transform infrared spectroscopy (FT-IR, IFS-66/S, Broker, MA), respectively. The surface topology of the GS assembled film was investigated using atomic force microscopy (AFM, Dimension 3100, Veeco, Plainview, NY) in tapping mode under dry condition. To visualize the shape characteristics of an individual GS, the GS dispersed solution was drop-dispensed onto a wafer substrate and dried for AFM observation. The film thickness of LbL assembled GSs was also measured with AFM (using a software of section analysis) after scratching the surface with a razor blade. The sheet resistance was measured with a linear-type four-point probe station (SR4−6 L, Modu systems, Korea) after thermal treatment of the assembled graphene thin films (trimmed size of sample = 1 cm × 1 cm).

RESULTS AND DISCUSSION

The GOs obtained from graphite powder have carboxyl and carbonyl groups at the edges and epoxide and phenolic hydroxyl functional groups on the basal plane.[48,49] Because of the plurality of carboxyl and epoxide functionalities, GOs are hydrophilic and intrinsically negatively charged. In addition, the exfoliated GO platelets can be converted to GS in which the epoxide groups on the plane are selectively removed through a chemical reduction process with hydrazine. In the course of this process, the hydrophilic nature of GO may be partially converted to hydrophobicity due to a considerable loss of epoxide groups; this may result in relatively poor dispersibility in aqueous conditions. A stably dispersed GS phase can be obtained through the deprotonation of carboxylic acid groups at the edges of the GS through pH control of the GS dispersion.[50] Or, this can be achieved via an addition of polymeric surfactant to the GS in order to provide a charged characteristic.[51] Therefore, the overall dispersibility of negatively charged GS can be primarily controlled by the charge strength of the remaining carboxyl groups whose pK_a is ∼4.2,

Scheme 1. Sequential Steps for the Amidation of Carboxylic Acid-Functionalized Graphene Oxide Platelets (to form an intermediate for further reaction with ethylenediamine, thionyl chloride is employed in the mid-process to generate the functions of acid chloride)

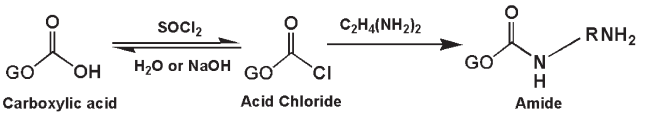

below which aggregation between GSs may occur. Therefore, to maintain the charged characteristic of carboxylic acid-functionalized GS, it is recommended that the pH be higher than the pK_a. This is further confirmed by the zeta potential measurements described later.

Similar to the synthesis of the negatively charged GS from GO, the carboxyl groups available in GO can be replaced with other functional groups to create positive charges on the surface of GS. As shown in Scheme 1, the carboxylic acid group on the edge of the GO can be converted to acid chloride group through the application of the strong reaction agent of thionyl chloride. This group, through a reaction with ethylenediamine, is then replaced with an amide group including a primary amine. This synthetic strategy has been widely accepted for the amidation process of nanocarbon materials, as demonstrated in carbon nanoparticles[52] and carbon nanotubes.[36] However, it has been very recently reported for graphene materials,[53,54] primarily because of difficulty in dispersing the GOs in reaction solvents. To use thionyl chloride as the reaction solvent for acyl-chlorination, the moisture remained in carboxylic acid-functionalized GOs obtained via Hummer's method should be completely removed. However, a drying process of fully exfoliated GOs after a sonication process

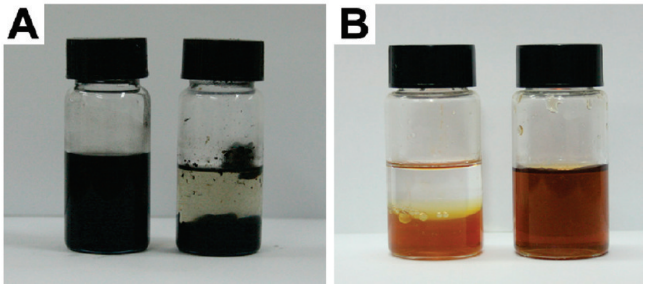

Figure 2. Dispersibility of graphite oxides (GOs) in thionyl chloride for acyl-chlorination reaction and in organic solvents for amidation reaction. (A) GOs dispersed in $SOCl_2$ solution after treatment with nonsonicated drying (powder phase, left) and with sonicated exfoliation and subsequent drying (aggregated film phase, right). (B) GOs dispersed in toluene (nonpolar, left) and pyridine (polar, right).

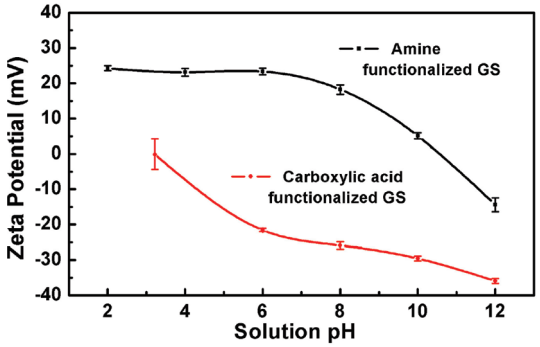

Figure 3. pH-dependent zeta potential of the functionalized GSs. Each zeta potential value was obtained by averaging the results of five samples synthesized from different batches. Error bars indicate the standard deviation.

results in a film phase aggregation of GOs; therefore, it exhibits poor solubility in thionyl chloride as shown in Figure 2A (right), eventually leading to a low yield in GS production. Because the employment of thionyl chloride for the acyl-chlorination reaction is basically targeted to carboxylic acid groups located at the edges of GO, not on the basal planes, we utilize nonsonicated GOs to prevent the aggregation of GOs after drying process. As a result, nonaggregated and powder phase GOs can be stably dispersed in thionyl chloride (Figure 2A, left). Another challenge associated with the solubility of GOs can be encountered during the amidation reaction of GOs through the addition of ethylenediamine. Unlike the carbon nanotube, which is capable of being dispersed in toluene solvent for amidation, the mixed characteristic between partial hydrophilicity and hydrophobicity of GOs does not allow for good dispersibility in nonpolar organic solvents (Figure 2B, left). Therefore, instead of using toluene, we adopted pyridine as a representative polar organic solvent, in which a good dispersibility during the amidation reaction can be obtained (Figure 2B, right).

As presented in Scheme 1, the formation of acid chloride from carboxylic acid through the reaction with thionyl chloride is a reversible reaction, and is likely accompanied by the reverse reaction in the presence of small amounts of water. Therefore, because of the simultaneously proceeding competing reactions, the obtained amine-functionalized graphenes inevitably contain some carboxylic acid groups. As a result, both negative and positive charges are simultaneously embedded on the edges of GS, yielding an amphoteric characteristic; thus the charged condition of GS can be switched between cationic and anionic characteristic according to the pH condition of the amine-functionalized GS dispersion. A zeta potential measurement was adopted to monitor the charged characteristic of the colloidal GS and the results are summarized in Figure 3.

As shown in Figure 3, the carboxylic acid-functionalized GS is always negatively charged in pH regimes above 3.2. Below pH 3.2, protonated and accordingly neutralized carboxylic acid-functionalized graphenes are irreversibly aggregated with one another. This result is consistent with the above discussion regarding the influence of the pK_a value of the carboxylic acid group on the aggregation of GSs, in which a pH value lower than 4.2 is expected to be a borderline value for the aggregation of carboxylic acid-functionalized GSs. On the other hand, the amine-functionalized GS shows positively charged characteristics in pH regimes below ~10.0. However, under higher pH conditions, amphoteric characteristics arise due to the residual carboxylic acid groups; namely, all amines are neutralized, whereas residual carboxylic acid groups can be deprotonated. As a result, a negatively charged characteristic is manifested under higher pH conditions. As can be captured from Figure 3, the isoelectric point (pI) of the amine-functionalized GS is 10.7. Similarly, this amphoteric behavior can be found elsewhere in the LbL assembly of polyampholytes.[55]

To assess the relative composition of constituting atoms and to obtain chemical information on synthesized GSs, we performed EDS and FT-IR characterizations. The results of EDS analysis shown in Table 1 reveal that the reduction of GO with hydrazine significantly decreases the oxygen content due to removal of an epoxide group, accordingly increasing the C/O ratio. Notably, a small amount of nitrogen exists in the carboxylic acid-functionalized GS, possibly due to a small addition of hydrazine as a reducing agent.[8] In contrast, the two-step amidation process that entails the intermediate addition of acyl chloride group and the loss of carboxylic acid groups drives enhancements in nitrogen and chlorine content, at the expense of a further decrease in oxygen content. Although chlorine atoms are present in only small concentration, they can be potentially beneficial for enhancing the electrical conductivity of the graphene film through creation of the p-type doping effect due to their strong electronegativity, accordingly increasing the hole density in the GS.[56,57] The atomic composition data obtained from EDS, in conjunction with the results from FT-IR characterization, can assist in the verification of the existence of specific chemical functionalities. Because a broad absorption peak of hydroxyl group is commonly observed for all samples at ν = 3000−3500 cm^{-1}, characteristic peaks located at the region of smaller wavenumbers were mainly investigated. As shown in Figure 4, the peak of the epoxide group at ν = 858 cm^{-1} (epoxy ring mode) typically observed from GO is absent after the chemical reduction process.[54] However, the peak of the carbonyl group (C═O stretching) from carboxylic acid at ν = 1730 cm^{-1} remains after the reduction reaction.[21] Furthermore, a successful amidation process to obtain the amine-functionalized GS can be verified from characteristic peaks at ν = 800 and 1070 cm^{-1} (NH_2 wagging) attributed to the amine group, and at ν = 1517 cm^{-1} of C−N−H (−C−H stretching; −C−N−H deformation) and ν = 1675 cm^{-1} of C═O (−C═O stretching in primary amides), indicative of an amide group.

Next, to elucidate the shape characteristics of the functionalized GSs, atomic force microscopic (AFM) observation was

Table 1. Energy-Dispersive Spectrometer (EDS) Measurements of GO and Functionalized GSs

	C (at %)	N (at %)	O (at %)	S (at %)	Cl (at %)	C/N ratio	C/O ratio
graphite Oxide	62.7		34.5	2.8			1.8
carboxylic acid-functionalized GS	76.5	7.4	15.7	0.4		10.4	4.9
amine-functionalized GS	71.3	17.6	8.7	1.9	0.5	4.0	8.2

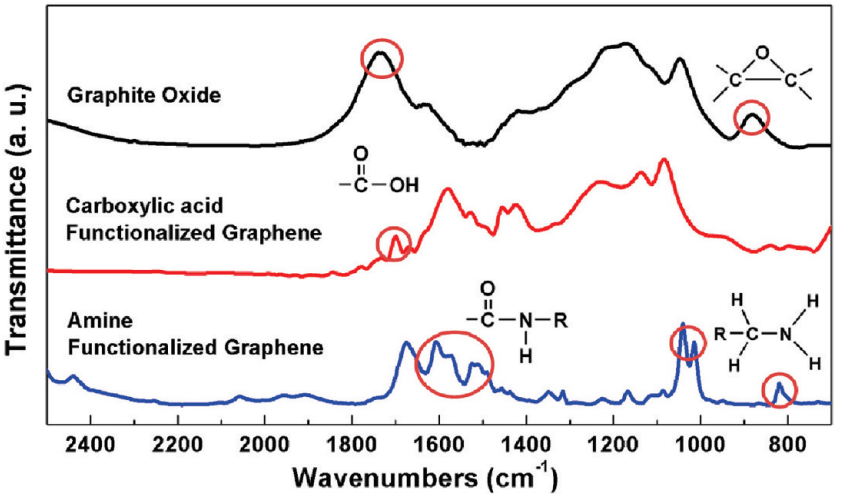

Figure 4. FT-IR spectra (700−2500 cm^{-1}) of GO and functionalized GSs. The auxiliary chemical formulas are added to denote important functional groups. Samples prepared on silicon substrate were measured in reflectance mode.

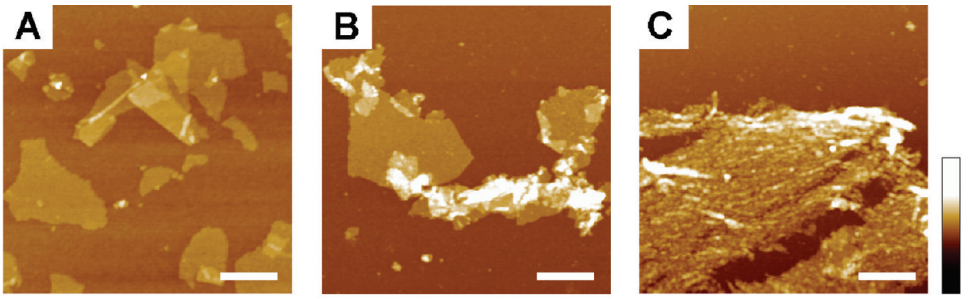

Figure 5. Atomic force microscopic observation of the functionalized GSs. The scale bar indicates 500 nm. (A) Platelet structure of negatively charged and carboxylic acid-functionalized GSs. Z-scale is 20 nm. (B, C) Structures of positively charged and amine-functionalized GSs: (B) folded and (C) textured. Z-scale in B and C is 50 nm.

performed. For a clear visualization of the two-dimensional sheet structure of graphene, diluted solutions of functionalized GSs (0.0025 wt %, 1/20 dilution of the original GS dispersion) were drop-cast onto the ultraflat substrate of a silicon wafer. As seen in Figure 5A, negatively charged GSs show a perfect platelet structure with a height of 1 ± 0.1 nm. On the other hand, the consecutive reactions of acyl-chlorination and the chemical reduction during fabrication of the amine-functionalized GS bring about a concomitant structural deformation in the GSs. As shown in Figures 5B and 5C, the positively charged and amine-functionalized GSs are deformed into folded or textured structures. Generation of these kinds of defect has not been reported upon using the same approach for the functionalization of CNTs[36,41] and can be attributed to the vigorous reaction of thionyl chloride with epoxide groups and phenolic hydroxyl groups in GSs, in which a thin two-dimensional geometry is more susceptible to deformation than the one-dimensional form. For example, some chloride functions on the basal plane of GS may induce electrostatic attractions with the primary amine groups located at the edges, likely leading to generation of a folded structure (Figure 5B). When the epoxide groups on the GS surface are scissored and removed by thionyl chloride, the platelet-like flat structure of GS is collapsed and some textures or wrinkles develop on the GS surface (Figure 5C).

Although a structural deficiency is observed for the amine-functionalized GSs, their charged characteristics can enable the LbL deposition and complexation with carboxylic acid-functionalized GSs. In addition, multiple numbers of charged groups are present on the edges of the functionalized GSs. Therefore, this characteristic of the polyvalency can readily allow for a LbL deposition between GSs. Notably, to obtain complementarily switched opposing charges of functionalized GSs for the LbL assembly process, the deposition condition was adjusted to pH 2.0 for the amine-functionalized GS and pH 8.0 for the carboxylic acid-functionalized GS, as determined from the zeta potential data in Figure 3. As a result, successful film deposition was achieved by varying the deposition numbers of GSs. As seen in Figure 6A, the film growth characteristic shows a linear

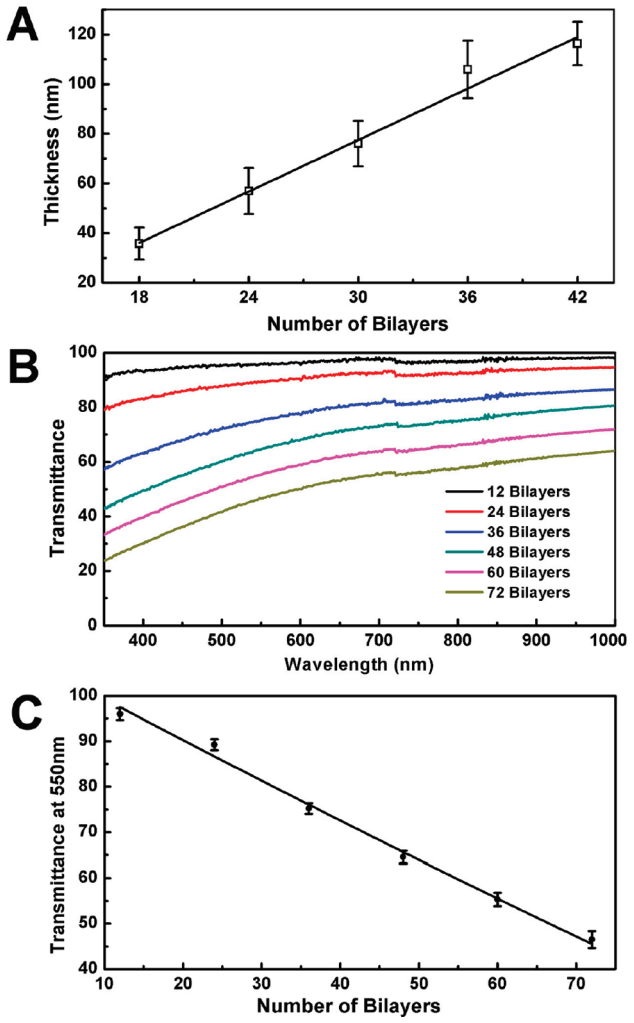

Figure 6. Film properties of the LbL-assembled GSs. (A) Thicknesses of graphene thin films with varying numbers of LbL depositions. The solid line is a linear fit and the error bars indicate the standard deviations. (B) Transparency spectra of graphene assembled thin films. (C) Light transmittance of graphene assembled thin films at a wavelength of 550 nm. The solid line is a linear fit and the error bars indicate the standard deviations.

proportionality in response to the LbL deposition number. However, if this linearity is valid over an entire regime of film deposition numbers (extrapolation of the linear plot), prominent film growth might initiate around 10 bilayer depositions, suggesting that the experimental adsorption rate of GS onto the substrate is retarded to some extent during the earlier period of LbL assembly. This effect can be attributed to the fact that the initial adsorption of GSs may not take place uniformly over the entire surface. Instead, as confirmed by AFM images in Figure 5 (or in Figure 7A), the adsorption of GS initially occurs in only partial areas of the surface, gradually propagating over the entire area. For example, the LbL-assembled film with 12 bilayers still lacks the surface uniformity, thus it shows a relatively large surface roughness compared to the film thickness, which makes it difficult to define the average film thickness accurately. This characteristic is indicative of a need for a predeposition of a number of bilayers to ensure the stabilized and completely covered film growth upon using LbL assembly.

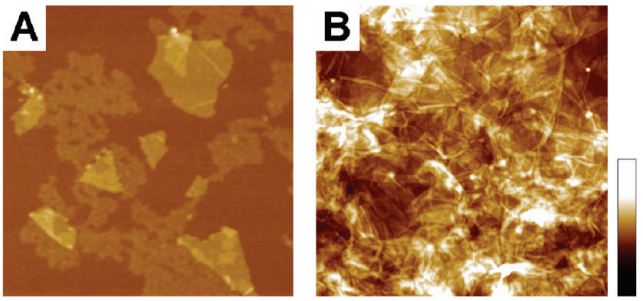

Figure 7. Atomic force microscopic observation of the LbL-assembled films of functionalized GSs. GSs are assembled on the plasma treated silicon wafer. Scan size is 2.5 μm × 2.5 μm. (A) $GS_{1.0}$ assembled film. Z-scale is 20 nm. (B) $GS_{12.0}$ assembled film. Z-scale is 50 nm.

In Figure 6A, the stepwise increment for bilayer deposition is observed to be around 3−4 nm. Because the thickness of a single layer of graphene is known to be 1 nm, a theoretical bilayer thickness should be 2 nm under ideal condition of stacking layers. However, as previously discussed, the fractional contribution to the increase in film thickness can differ according to the type of GS functionality. For the amine-functionalized GS, structural deformations such as folding or texturing that occur due to generation of surface defect lead to a subsequent increase in the stepwise thickness during LbL deposition. Light transmittance data for LbL-assembled graphene films are presented in Figure 6B. A good film transparency with >80% in transmittance is observed for LbL-assembled films with deposition numbers less than 24 bilayers, approximately equal to 60 nm in film thickness. It is generally known that an increase in the stacking of a single graphene layer in the epitaxially grown graphene films (CVD method) causes an additional decrease in light transmittance of 2.3%.[58] Hence, to obtain a minimum of 80% transmittance, less than ten layers of stacking (approximately 10 nm in thickness) are required in the CVD process. However, compared with the full surface coverage of a single graphene layer in the CVD process, a film deposition method based on LbL assembly allows for GSs adsorption with partial surface coverage and incorporation of voids inside the films. These characteristics result in a considerably mitigated tendency in the light transmittance in response to an increase in LbL deposition numbers (Figure 6C), thus a relatively thicker film prepared using this method can exhibit an optical transparency similar to that of a much thinner film prepared using CVD process.

The sequential stacking of GSs by LbL deposition can also be confirmed through AFM characterization. Figure 7 shows surface morphologies of GS assembled films for 1.0 bilayer (left) and 12.0 bilayers (right). Here, it should be noted that the image of the 1.0 bilayer deposition shown in Figure 7A has two important implications with regard to the characteristics of LbL assembly of the functionalized GSs: structural defect generation in the positively charged GSs and partial adsorption of GSs onto the substrate in the earlier period of LbL assembly. Compared with a complete platelet structure of negatively charged GSs with a smooth plane and distinct edges, the positively charged GSs show a tattered surface with indistinctly developed edges, primarily due to the intense reactivity of the thionyl chloride solvent. Moreover, because the GSs lack a structural conformability upon adsorption to a flat substrate, complete adsorption of GSs over the entire surface can be obtained after a number of bilayer depositions, after which the substrate effect can be

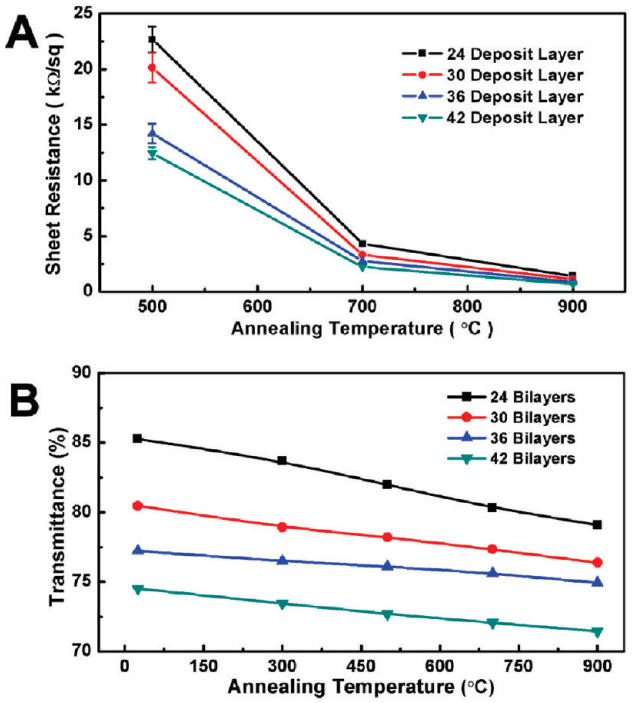

Figure 8. Film properties of the LbL-assembled graphene films after thermal annealing. (A) Sheet resistance of the LbL-assembled graphene thin films as a function of annealing temperature. (B) Gradual loss in film transparency in accordance with an increase in the film annealing temperature. The transparency is defined as the transmittance at a wavelength of 550 nm.

minimized. Once the LbL adsorption of GSs is stabilized, the film deposition follows a linear growth pattern in response to an increase in the deposition number, while maintaining a relatively flat surface. As shown in Figure 7B, after 12.0 bilayer adsorptions of the functionalized GSs, the root-mean-square (rms) roughness for the overall film surface is maintained at 5.6 nm.

If the assembled graphene thin films are to be utilized for practical electrical applications, a good electrical conductivity should be guaranteed. Because the graphene thin films that are chemically assembled via LbL deposition still contain a number of charged functional groups within the film, electron are prone to be trapped by these charged functionalities and the sheet resistance of a film is expected to be accordingly high. Under nontreated conditions, LbL assembled graphene films show a sheet resistance of hundreds of mega-ohms/sq. Therefore, a thermal treatment process under an Ar environment can be employed to remove these functional groups and enhance the electrical conductivity. In the case of GOs, it has been reported that the thermal removal of epoxide groups on the basal plane while adding hydrogen gas can cause the serious defect generation on the GS surface, such that the sheet resistance of the graphene film actually increases, contrary to one's expectation.[23] However, in our system, GSs that have been previously chemically reduced are subject to an additional thermal treatment process, during which fewer defects are likely generated and well-interconnected random networks within multilayered GSs are to be developed, resulting in a desirable decrease in sheet resistance. As shown in Figure 8A, the sheet resistance of the LbL-assembled graphene films decreases in accordance with an increase in the annealing temperature, indicative of the effectiveness of thermal treatment in removing the residual functionalities within the films.

In addition, thermal treatment process can affect the transparency as well as the sheet resistance of the film. The results presented in Figure 8B show a gradual loss in light transmittance with increasing thermal annealing temperature. This can be attributed to the fact that the proliferated sp^2 binding between stacked graphene nanosheets upon thermal annealing results in a slight decrease in the light transmittance of a film.[49] It should be noted that there is no noticeable thickness reduction even after thermal annealing process, implying that a possibility of the film densification and subsequent transmittance reduction due to the loss of organic functionalities can be negated. In this study, an additional transparency loss of 4−5% at a wavelength of 550 nm is generally observed for the LbL-assembled graphene thin films after thermal annealing. As a result, the lowest sheet resistance obtained from experiments was 700 Ω/sq for the $GS_{42.0}$ deposited film with a light transmittance of 72% at a wavelength of 550 nm. However, to meet the minimum requirement of 80% light transmittance for a practical transparent electrode application, a sheet resistance of 1.4 kΩ/sq from the $GS_{24.0}$ deposited film was the best result in this study. The obtained sheet resistance is considerably lower than the values previously reported for chemically self-assembled graphene hybrid systems. The Langmuir−Blodgett assembled films consisting of chemically modified graphenes yielded a sheet resistance of 8 kΩ/sq at a transparency of 83% and vacuum filtered films of graphene platelets showed a sheet resistance of 3 kΩ/sq at a transparency of 75%.[23,59] In our system, because of incorporation of acyl chloride groups during the reaction with thionyl chloride, a p-doping effect can be projected onto the assembled graphene films, yielding an enhanced sheet resistance. Because of their strong electronegativity, the acyl-chlorinated functional group acts as electron acceptor, tending to increase the hole density in GSs. Therefore, acyl-chlorinated functional groups are able to improve the electron-transport properties of GSs.[56,57]

CONCLUSIONS

A sequentially stacked and chemically assembled graphene thin film can be fabricated using layer-by-layer assembly of oppositely charged graphene nanosheets. Stably dispersed aqueous solutions of the functionalized graphenes can be generated by chemical reduction of the graphene oxide nanoplatelets. Unlike other studies in which positively charged graphenes have shown low dispersibility in water, in this study, a modification to thionyl chloride chemistry during the functionalization of graphene nanosheets enabled a successful amidation process without sacrificing the advantage of good aqueous dispersibility. As a result, through the alternate layer-by-layer assembly between amine-functionalized and carboxylic acid-functionalized graphene nanosheets, uniformly assembled graphene thin films were constructed, offering full controllability of both film thickness and light transmittance. The deposited graphene thin films were further thermally reduced for improved electrical characteristics, resulting in a sheet resistance of 1.4 kΩ/sq for a light transmittance of 80%. This approach for fabricating layer-by-layer assembled graphene thin film is highly advantageous in that all procedures are performed in all aqueous environments, which is environmentally benign and highly compatible to an industrial scale-up process. At the same time, it can provide full capability for manipulating the physical/electrical properties of thin films,

including film thickness, sheet resistance, and light transparency, and thus, it is anticipated to be useful in various electrical, optical, and biological applications.

AUTHOR INFORMATION

Corresponding Author
*E-mail: pjyoo@skku.edu.

ACKNOWLEDGMENT

This work was supported by Basic Science Research Program grants (2010-0009877, 2010-0027771, 2010-0029409) and research grant (NRF-C1AAA001-2010-0028958) through the National Research Foundation of Korea (NRF) funded by the Korea Government (MEST).

REFERENCES

(1) Rao, C. N. R.; Biswas, K.; Subrahmanyam, K. S.; Govindaraj, A. *J. Mater. Chem.* **2009,** *19,* 2457–2469.
(2) Geim, A. K.; Novoselov, K. S. *Nat. Mater.* **2007,** *6,* 183–191.
(3) Novoselov, K. S.; Jiang, D.; Schedin, F.; Booth, T. J.; Khotkevich, V. V.; Morozov, S. V.; Geim, A. K. *Proc. Nat. Acad. Sci. U.S.A* **2005,** *102,* 10451–10453.
(4) Somani, P. R.; Somani, S. P.; Umeno, M. *Chem. Phys. Lett.* **2006,** *430,* 56–59.
(5) Kim, K. S.; Zhao, Y.; Jang, H.; Lee, S. Y.; Kim, J. M.; Kim, K. S.; Ahn, J.-H.; Kim, P.; Choi, J.-Y.; Hong, B. H. *Nature* **2009,** *457,* 706–710.
(6) Reina, A.; Jia, X. T.; Ho, J.; Nezich, D.; Son, H. B.; Bulovic, V.; Dresselhaus, M. S.; Kong, J. *Nano Lett.* **2009,** *9,* 30–35.
(7) Tung, V. C.; Allen, M. J.; Yang, Y.; Kaner, R. B. *Nat. Nanotechnol.* **2009,** *4,* 25–29.
(8) Stankovich, S.; Dikin, D. A.; Piner, R. D.; Kohlhaas, K. A.; Kleinhammes, A.; Jia, Y.; Wu, Y.; Nguyen, S. T.; Ruoff, R. S. *Carbon* **2007,** *45,* 1558–1565.
(9) Lee, J. H.; Shin, D. W.; Makotchenko, V. G.; Nazarov, A. S.; Fedorov, V. E.; Kim, Y. H.; Choi, J.-Y.; Kim, J. M.; Yoo, J.-B. *Adv. Mater.* **2009,** *21,* 4383–4387.
(10) Li, D. S.; Windl, W.; Padture, N. P. *Adv. Mater.* **2009,** *21,* 1243–1246.
(11) Kosynkin, D. V.; Higginbotham, A. L.; Sinitskii, A.; Lomeda, J. R.; Dimiev, A.; Price, B. K.; Tour, J. M. *Nature* **2009,** *458,* 872–876.
(12) Jiao, L. Y.; Zhang, L.; Wang, X. R.; Diankov, G.; Dai, H. J. *Nature* **2009,** *458,* 877–880.
(13) Si, Y.; Samulski, E. T. *Nano Lett.* **2008,** *8,* 1679–1682.
(14) Wang, G. X.; Yang, J.; Park, J.; Gou, X. L.; Wang, B.; Liu, H.; Yao, J. *J. Phys. Chem. C* **2008,** *112,* 8192–8195.
(15) Muszynski, R.; Seger, B.; Kamat, P. V. *J. Phys. Chem. C* **2008,** *112,* 5263–5266.
(16) Schniepp, H. C.; Li, J. L.; McAllister, M. J.; Sai, H.; Herrera-Alonso, M.; Adamson, D. H.; Prud'homme, R. K.; Car, R.; Saville, D. A.; Aksay, I. A. *J. Phys. Chem. B* **2006,** *110,* 8535–8539.
(17) McAllister, M. J.; Li, J. L.; Adamson, D. H.; Schniepp, H. C.; Abdala, A. A.; Liu, J.; Herrera-Alonso, M.; Milius, D. L.; Car, R.; Prud'homme, R. K.; Aksay, I. A. *Chem. Mater.* **2007,** *19,* 4396–4404.
(18) Williams, G.; Seger, B.; Kamat, P. V. *ACS Nano* **2008,** *2,* 1487–1491.
(19) Bourlinos, A. B.; Gournis, D.; Petridis, D.; Szabo, T.; Szeri, A.; Dekany, I. *Langmuir* **2003,** *19,* 6050–6055.
(20) Stankovich, S.; Dikin, D. A.; Dommett, G. H. B.; Kohlhaas, K. M.; Zimney, E. J.; Stach, E. A.; Piner, R. D.; Nguyen, S. T.; Ruoff, R. S. *Nature* **2006,** *442,* 282–286.
(21) Xu, Y.; Liu, Z.; Zhang, X.; Wang, Y.; Tian, J.; Huang, Y.; Ma, Y.; Zhang, X.; Chen, Y. *Adv. Mater.* **2009,** *21,* 1275–1279.
(22) Geng, J.; Jung, H. *J. Phys. Chem. C* **2010,** *114,* 8227–8234.
(23) Li, X. L.; Zhang, G. Y.; Bai, X. D.; Sun, X. M.; Wang, X. R.; Wang, E.; Dai, H. J. *Nat. Nanotechnol.* **2008,** *3,* 538–542.
(24) Cote, L. J.; Kim, F.; Huang, J. *J. Am. Chem. Soc.* **2008,** *131,* 1043–1049.
(25) Eda, G.; Fanchini, G.; Chhowalla, M. *Nat. Nanotechnol.* **2008,** *3,* 270–274.
(26) Kong, B. S.; Geng, J. X.; Jung, H. T. *Chem. Commun.* **2009,** 2174–2176.
(27) Geng, J.; Jung, H. T. *J. Phys. Chem. C* **2010,** *114,* 8227–8234.
(28) Zhu, Y. W.; Cai, W. W.; Piner, R. D.; Velamakanni, A.; Ruoff, R. S. *Appl. Phys. Lett.* **2009,** *95,* 103104.
(29) Decher, G. *Science* **1997,** *277,* 1232–1237.
(30) Hammond, P. T. *Adv. Mater.* **2004,** *16,* 1271–1293.
(31) Caruso, F.; Caruso, R. A.; Mohwald, H. *Science* **1998,** *282,* 1111–1114.
(32) Lee, D.; Rubner, M. F.; Cohen, R. E. *Nano Lett.* **2006,** *6,* 2305–2312.
(33) Yoo, P. J.; Nam, K. T.; Qi, J. F.; Lee, S. K.; Park, J.; Belcher, A. M.; Hammond, P. T. *Nat. Mater.* **2006,** *5,* 234–240.
(34) Berg, M. C.; Yang, S. Y.; Hammond, P. T.; Rubner, M. F. *Langmuir* **2004,** *20,* 1362–1368.
(35) Mamedov, A. A.; Kotov, N. A.; Prato, M.; Guldi, D. M.; Wicksted, J. P.; Hirsch, A. *Nat. Mater.* **2002,** *1,* 190–194.
(36) Lee, S. W.; Kim, B. S.; Chen, S.; Shao-Horn, Y.; Hammond, P. T. *J. Am. Chem. Soc.* **2009,** *131,* 671–679.
(37) Cassagneau, T.; Guerin, F.; Fendler, J. H. *Langmuir* **2000,** *16,* 7318–7324.
(38) Vickery, J. L.; Patil, A. J.; Mann, S. *Adv. Mater.* **2009,** *21,* 2180–2184.
(39) Kovtyukhova, N. I.; Ollivier, P. J.; Martin, B. R.; Mallouk, T. E.; Chizhik, S. A.; Buzaneva, E. V.; Gorchinskiy, A. D. *Chem. Mater.* **1999,** *11,* 771–778.
(40) Cassagneau, T.; Fendler, J. H. *J. Phys. Chem. B* **1999,** *103,* 1789–1793.
(41) Hong, T.-K.; Lee, D. W.; Choi, H. J.; Shin, H. S.; Kim, B.-S. *ACS Nano* **2010,** *4,* 3861–3868.
(42) Wu, J. H.; Tang, Q. W.; Sun, H.; Lin, J. M.; Ao, H. Y.; Huang, M. L.; Huang, Y. F. *Langmuir* **2008,** *24,* 4800–4805.
(43) Tang, Q.; Wu, J.; Li, Q.; Lin, J. *Polymer* **2008,** *49,* 5329–5335.
(44) Niyogi, S.; Bekyarova, E.; Itkis, M. E.; McWilliams, J. L.; Hamon, M. A.; Haddon, R. C. *J. Am. Chem. Soc.* **2006,** *128,* 7720–7721.
(45) Shen, J. F.; Hu, Y. Z.; Li, C.; Qin, C.; Shi, M.; Ye, M. X. *Langmuir* **2009,** *25,* 6122–6128.
(46) Fang, Y. X.; Guo, S. J.; Zhu, C. Z.; Zhai, Y. M.; Wang, E. K. *Langmuir* **2010,** *26,* 11277–11282.
(47) Hummers, W. S.; Offeman, R. E. *J. Am. Chem. Soc.* **1958,** *80,* 1339–1339.
(48) Bagri, A.; Mattevi, C.; Acik, M.; Chabal, Y. J.; Chhowalla, M.; Shenoy, V. B. *Nat Chem, 2,* 581-587.
(49) Mattevi, C.; Eda, G.; Agnoli, S.; Miller, S.; Mkhoyan, K. A.; Celik, O.; Mastrogiovanni, D.; Granozzi, G.; Garfunkel, E.; Chhowalla, M. *Adv. Funct. Mater.* **2009,** *19,* 2577–2583.
(50) Li, D.; Muller, M. B.; Gilje, S.; Kaner, R. B.; Wallace, G. G. *Nat. Nanotechnol.* **2008,** *3,* 101–105.
(51) Stankovich, S.; Piner, R. D.; Chen, X. Q.; Wu, N. Q.; Nguyen, S. T.; Ruoff, R. S. *J. Mater. Chem.* **2006,** *16,* 155–158.
(52) Zhu, J. Z.; Deng, B. L.; Yang, J.; Gang, D. C. *Carbon* **2009,** *47,* 2014–2025.
(53) Hu, Y.; Shen, J.; Li, N.; Ma, H.; Shi, M.; Yan, B.; Huang, W.; Wang, W.; Ye, M. *Compos. Sci. Technol.* **2010,** *70,* 2176–2182.
(54) Hu, Y.; Shen, J.; Li, N.; Shi, M.; Ma, H.; Yan, B.; Wang, W.; Huang, W.; Ye, M. *Polym. Compos.* **2010,** *31,* 1987–1994.
(55) Chen, G.; Wu, G. J.; Wang, L. M.; Zhang, S. B.; Su, Z. H. *Chem. Commun.* **2008,** 1741–1743.
(56) Parekh, B. B.; Fanchini, G.; Eda, G.; Chhowalla, M. *Appl. Phys. Lett.* **2007,** *90,* 121913.

(57) Eda, G.; Lin, Y.-Y.; Miller, S.; Chen, C.-W.; Su, W.-F.; Chhowalla, M. *Appl. Phys. Lett.* **2008,** *92*, 233305.
(58) Nair, R. R.; Blake, P.; Grigorenko, A. N.; Novoselov, K. S.; Booth, T. J.; Stauber, T.; Peres, N. M. R.; Geim, A. K. *Science* **2008,** *320*, 1308.
(59) De, S.; King, P. J.; Lotya, M.; O'Neill, A.; Doherty, E. M.; Hernandez, Y.; Duesberg, G. S.; Coleman, J. N. *Small* **2010,** *6*, 458–464.